International Journal of Steel Structures 16(4): 1319-1327 (2016)
DOI 10.1007/s13296-016-0045-4
ISSN 1598-2351 (Print)
ISSN 2093-6311 (Online)

International Journal of
STEEL
STRUCTURES
www.springer.com/journal/13296

Extending Fatigue Life of Out-of-plane Gusset Joint by Bonding CFRP Plates Under Bending Moment

Risa Matsumoto[1,*], Toshiyuki Ishikawa[2], Manabu Takemura[3], Yoshisato Hiratsuka[4], and Hirotaka Kawano[4]

[1]*Assistant Professor, Department of Urban Management, Kyoto University, Kyotodaigaku-katsura, Nishikyo-ku, Kyoto 615-8540, Japan*
[2]*Associate Professor, Department of Civil, Environmental, and Applied System Engineering, Kansai University, 3-3-35 Suita-shi Yamate-cho, Osaka 564-8680, Japan*
[3]*Technical Research Institute, SHO-BOND Corporation, 1-17 sakura Tsukuba-shi, Ibaragi, Japan*
[4]*Head Office, SHO-BOND Corporation, 7-8 Nihonbashi Hakozaki-cho, Chuo-ku, Tokyo, Japan*
[5]*Professor, Department of Urban Management, Kyoto University, Kyotodaigaku-katsura, Nishikyo-ku, Kyoto 615-8540, Japan*

Abstract

Carbon fiber reinforced plastic, CFRP, plates bonding method is one of the new repair methods for fatigue cracks. In this method, propagation of fatigue crack will be delay because of the suppression of crack opening by crack bridging and stress reduction by composite effect of bonding CFRP plates. In this study, to clarify the effect of bonding CFRP plates on fatigue life extension, bending fatigue tests were carried out. First, fatigue tests on the specimens in as-welded condition were conducted until fatigue crack propagated to 10mm away from the weld toe. Then, fatigue crack was covered by CFRP plates and the specimens were re-tested until fatigue crack penetrated through the base plate. As the results of bending fatigue tests, the fatigue test data of the specimens repaired by bonding CFRP plates showed much longer fatigue life compared with that in as-welded condition, under stress ratio, R=0 and -infinity.

Keywords: CFRP plate, out-of-plane gusset joint, fatigue strength, bending moment

1. Introduction

It is reported that many fatigue cracks are initiated from weld toes in steel girders, orthotropic steel deck plates and steel piers. Fatigue cracks are often repaired tentatively by stop-holes which are the holes drilled at the crack tips. If the crack tips are completely removed by stop-holes, fatigue life will be extended. However, since the stop-holes make defects of cross sectional areas of steel members, nominal stress becomes higher than that in the intact one. Recently, carbon-fiber reinforced plastic (CFRP) plates have been used for the tentative repair of fatigue cracks (National Research Council, 2007; Chacon *et al*., 2004; Phares *et al*., 2003; and, Roach *et al*., 2008). The CFRP plate has excellent material properties with lower weight, and also applicable for rapid repairs. Moreover, this method in which CFRP plates are bonded on fatigue cracks does not make defects of any cross sectional areas in the steel members.

In the previous study, the effect of bonding CFRP plates on fatigue life extension was already clarified. For instance, Colombi and Liu focused on a stress intensity factor (SIF) of a single plane-plate with through crack under tensile loading and they had proposed the SIF of a crack covered by bonding CFRP plates (Colombi, 2005; Liu *et al*., 2009). Nakamura conducted tensile fatigue tests using out-of-plane gusset specimens repaired by CFRP plates to clarify the effect on fatigue life extension by bonding CFRP plates in the welded structures (Nakamura *et al*., 2011).

Most studies, however, focused on the extended fatigue life by bonding CFRP plates under tensile cyclic loading. In the existing structures, however, the larger secondary stress caused by out-of-plane bending moment was introduced, such as orthotropic steel deck plate. Therefore, the purpose of this study is to confirm the effect of bonding CFRP plates, which is tentative repair, on fatigue life extension under cyclic bending moment by conducting plate bending fatigue tests.

Received January 29, 2016; accepted August 22, 2016;
published online December 31, 2016

*Corresponding author
Tel: +81-(0)75-383-3321, Fax: +81-(0)75-383-3324
E-mail: matsumoto.risa.8z@kyoto-u.ac.jp

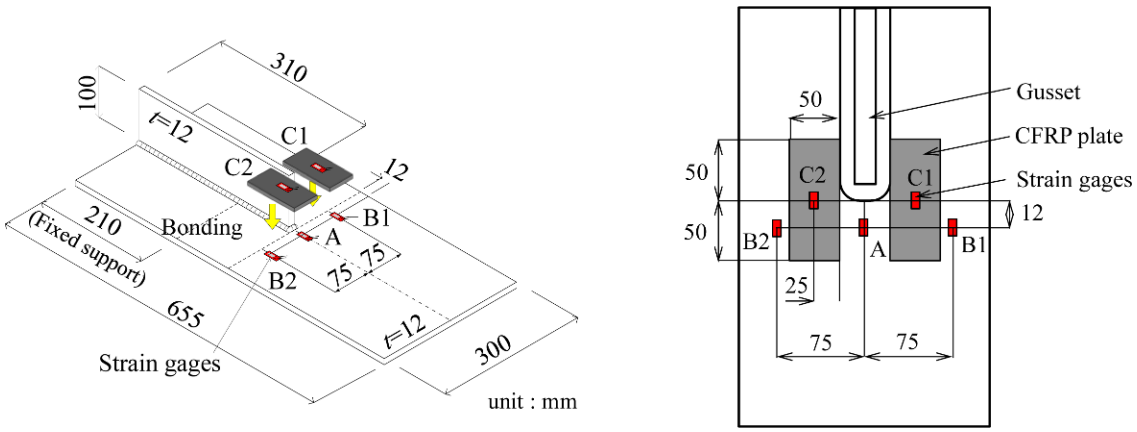

Figure 1. Test specimen.

Table 1. Mechanical properties and chemical composition of the steel plate (SM490Y)

σ_Y (N/mm^2)	σ_b (N/mm^2)	Elongation (%)	Chemical composition (%)				
			C	Si	Mn	P	S
409	536	25	0.15	0.40	1.41	0.016	0.003

2. Specimen and Fatigue Test

In the fatigue tests, out-of-plane gusset welded joints fabricated by using JIS-SM490YA, which has guaranteed yield stress of 355 N/mm^2 and tensile strength of 490 N/mm^2, were prepared (Fig. 1). The specimen was composed of the 12 mm thick gusset plate and the 12 mm thick base plate. The mechanical properties and chemical composition of JIS-SM490YA are listed in Table 1.

The fatigue test was carried out using the fatigue testing machine generating a plate bending type of loading, as shown in Fig. 2. A cantilever-type specimen was set on a frame bed and a vibrator was installed on the free end of the base plate to generate constant amplitude vibration which was transformed into a bending type of loading to apply a test specimen. Stress ranges were controlled by the vibration frequency, and defined as multiplication of elastic modulus and the initial average strain ranges of gages B1 and B2 (Fig. 1). Stress ratio, R, was controlled by the adjustment of springs installed at the free end of the specimen. In this study, stress ratio, R, at the weld toe was controlled as 0 by the adjustment of these springs which produced tensile stress to the specimen surface, or controlled as -infinity by the adjustment of these springs which produced compressive stress to the specimen surface.

Fatigue tests on the specimens in as-welded condition were conducted until fatigue crack propagated to 10 mm away from the weld toe (N_{10}), as illustrated in Fig. 2. Then, fatigue crack was repaired by bonding CFRP plates with acrylic resin under unloading condition (Fig. 1). The longitudinal elastic modulus of the CFRP plate is 450 kN/mm^2 and the elastic modulus of acrylic resin is 1.35 kN/mm^2. As described in Fig. 1, the dimension of the CFRP plate is 100 mm×50 mm×2.1 mm (longitudinal direction ×transverse direction×thickness direction). Steel plate surface where the CFRP plates were bonded after initiation of fatigue crack was finished by angle grinder with roughness number of #100. The location of strain gages are shown in Fig. 1. AW and N_{10}+CFRP specimens indicate the specimen in as-welded condition and the specimen repaired by using CFRP, respectively. To clarify the influence of curing time on the effectiveness of the fatigue extension, curing time were controlled as 2 hours and 2 weeks in the N_{10}+CFRP specimens under the stress range of $\Delta\sigma$=60 N/mm^2 and stress ratio, R=0. In the other N_{10}+CFRP specimens, curing time were controlled as over 2 weeks.

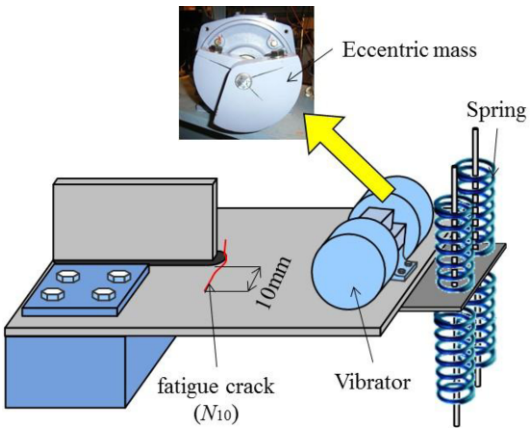

Figure 2. Test set up.

Table 2. Fatigue test results (stress ratio, R=0)

Specimen	State	Stress range (N/mm^2)	Fatigue life $N_{10}\rightarrow N_t$ ($\times 10^4$)
AW-1	As-welded	60.8	198.2
AW-2		99.9	16.0
N_{10}+CFRP-1	N_{10} crack +CFRP	57.5	1846.7
N_{10}+CFRP-2		57.8	2589.2
N_{10}+CFRP-3		80.2	376.8
N_{10}+CFRP-4		79.9	410.8
N_{10}+CFRP-5		101.8	56.8
N_{10}+CFRP-6		99.8	123.4
N_{10}+CFRP-7		130.0	35.7
N_{10}+CFRP-8		122.1	26.8

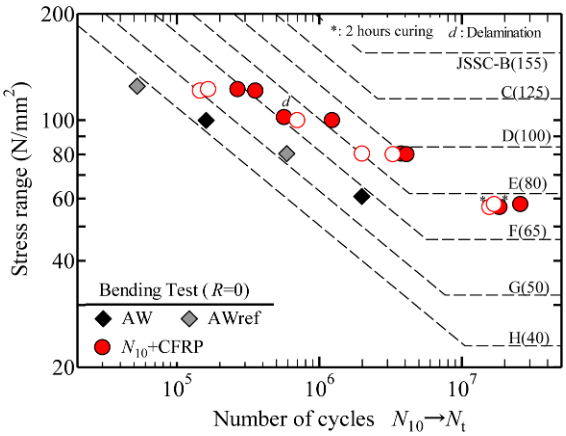

Figure 3. S-N curve (stress ratio, R=0).

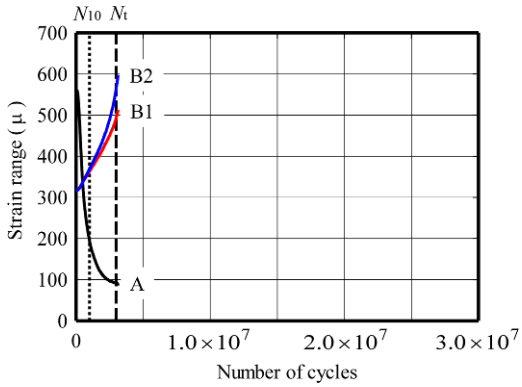

Figure 4. Variation of strain range in the AW specimen ($\Delta\sigma$=60 N/mm^2)

3. Fatigue Test Results (stress ratio, R=0)

3.1. S-N curve

The fatigue test results are listed in Table 2. Figure 3 shows the S-N diagram of the fatigue test results. In this fatigue test, after the repaired crack propagated to the thickness and width direction, the other crack initiated from the back surface of the specimen when the main crack propagated close to the back surface. Accordingly, fatigue life ($N_{10}\rightarrow N_t$) is defined as number of cycles after fatigue crack propagated to 10mm away from the weld toe (N_{10}) until fatigue crack initiated at the back surface of the specimens (N_t). Fatigue tests were conducted under the stress range of $\Delta\sigma$=60, 80, 100 or 120 N/mm^2 with stress ratio R=0, in each type of the specimens. In Fig. 3, fatigue lives of CFRP plate delamination, which are defined as number of cycles when the strain ranges at gages C1 and C2 began to decrease, are also plotted as white circles. As mentioned in latter chapter 3.3 (2), since for the N_{10}+CFRP specimen with "d", in which the edge of the CFRP plate could not be completely bonded, the delamination of the CFRP plate proceeded just after the fatigue test started. Therefore, fatigue life of CFRP plate delamination in the N_{10}+CFRP specimen with "d" is not plotted in Fig. 3. As seen in Fig. 3, in all specimens, fatigue crack appeared at the back surface of the specimen after the CFRP plates delaminated. The fatigue test result of the N_{10}+CFRP specimen with "d" showed shorter fatigue life compared with that of the other N_{10}+CFRP specimens. However, the fatigue lives of the N_{10}+CFRP specimens could be extended more than 4 times compared with those of the AW specimens under the stress range $\Delta\sigma$=60 to 120 N/mm^2, even if the initial delamination of CFRP plates was observed. Additionally, the extended fatigue life of the specimen with "*", in which adhesive is cured for 2 hours, is as long as that of the specimen cured for 2 weeks. Therefore, it is clear that the sufficient extension of fatigue life can be obtained when adhesion bond was cured for over 2 hours.

3.2. Variation of strain range during fatigue test

Variation of the strain ranges during the fatigue tests are shown in Figs. 4 to 6. Meanwhile, in Figs. 5 and 6, the strain ranges of the AW specimen under N_{10} condition at gages of A, B1 and B2 (AW, N_{10}), which are the strain ranges measured at the same specimen just before bonding CFRP plates, are also plotted as broken lines respectively. In the AW specimen as shown in Fig. 4, the strain range at gage A decreased and the strain ranges at gages B1 and B2 increased as fatigue crack initiated at the weld toe and propagated to the base plate.

Besides that, in Fig. 5(a), in the N_{10}+CFRP specimen with 2 hours curing, the strain ranges at gages C1 and C2 located on CFRP sharply increased in the initial stage of the fatigue test. This is because the adhesive strength was under developing after 2 hours curing. However, after the adhesive strength completely developed, the stress generated in the base plate could be transferred through the adhesive layer to the CFRP plates with the increase in the strain ranges on the CFRP plates. Therefore, the strain ranges at gages B1 and B2 located at the crack tips sharply decreased in the initial stage of the fatigue test after adhesive strength development. Furthermore, the strain ranges at gages B1 and B2 could be reduced 40% compared

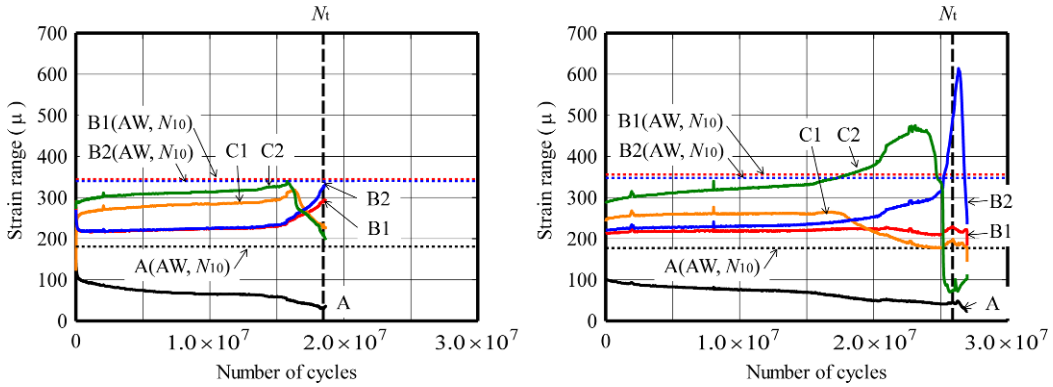

Figure 5. Variation of strain range in the N_{10}+CFRP specimen ($\Delta\sigma$=60 N/mm^2).

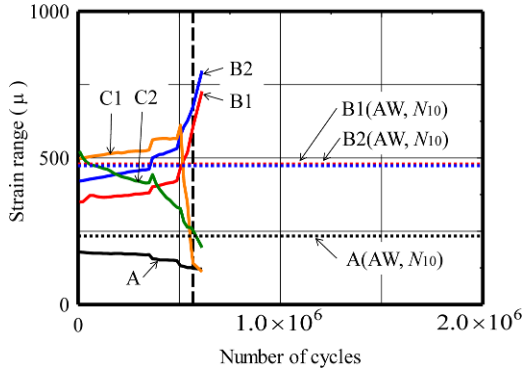

Figure 6. Variation of strain range in the N_{10}+CFRP specimen with CFRP delamination ($\Delta\sigma$=100 N/mm^2)

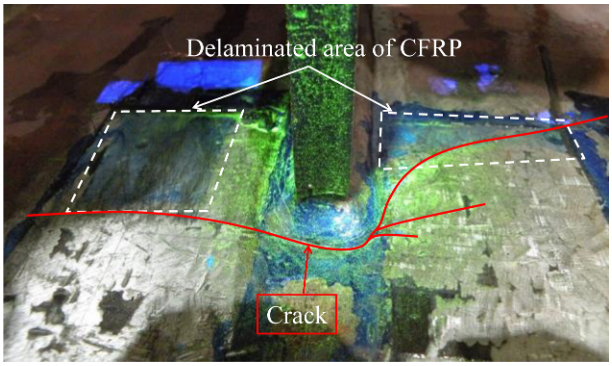

Figure 7. Delamination aria of CFRP.

with the AW specimen under N_{10} condition (AW, N_{10}). The strain range at gage A located near the weld toe could be also reduced compared with (AW, N_{10}) condition by bonding CFRP.

However, since the strain range at gage A gradually decrease, it can be assumed that fatigue crack gradually re-propagated on the surface of the base plate. The strain ranges at gages B1 and B2 located at the crack tips and the strain ranges at gages C1 and C2 located on the CFRP plates increased with fatigue crack propagation. Furthermore, the strain ranges at gages C1 and C2 dropped sharply at 17 million cycles. This implies that the CFRP plates began to delaminate at 17 million cycles. Variation of the strain ranges at gages B1 and B2 increased after the CFRP plates delaminated. Accordingly, it seems that the crack propagation velocity accelerated after the CFRP plates delaminated. Finally, fatigue crack initiated at the back surface of the specimen.

Figure 5(b) presents the N_{10}+CFRP specimen with adhesive cured for 2 weeks. As shown in Fig. 5(b), the strain range at gage A in the initial stage of the fatigue test could be reduced compared with (AW, N_{10}) condition. Therefore, it can be assumed that the adhesive strength had completely developed before fatigue test started. The strain ranges at gages B1 and B2 in the N_{10}+CFRP specimen in the initial stage of the fatigue test could be also reduced compared with (AW, N_{10}) condition. As can be seen in Fig. 5(b), the strain range at gage A gradually decreased with fatigue crack propagation. At the left side of the gusset plate, the strain ranges at gages B2 located at the crack tip and C2 located on the CFRP plate increased with fatigue crack propagation. Since the strain range at gage C2 significantly decreased at 25 million cycles, it can be assumed that the CFRP plate began to delaminate at 25 million cycles. On the contrary, at the right side of the gusset plate, the strain range at gage B1 located at crack tip was almost constant during fatigue test. The strain range at gage C1 located on the CFRP plate was also constant until 17 million cycles and decreased over 17 million cycles.

To clarify the difference of the strain range variation between the right and left sides of the gusset plate, the CFRP plates were removed after the fatigue test finished, and the direction of the crack propagation was investigated as presented in Fig. 7. At the right side of the gusset (gages B1 and C1), fatigue crack propagated largely in the diagonal direction against the gusset plate. Consequently, the strain ranges at gages B1 and C1 were almost constant even if the fatigue crack propagated. At the left

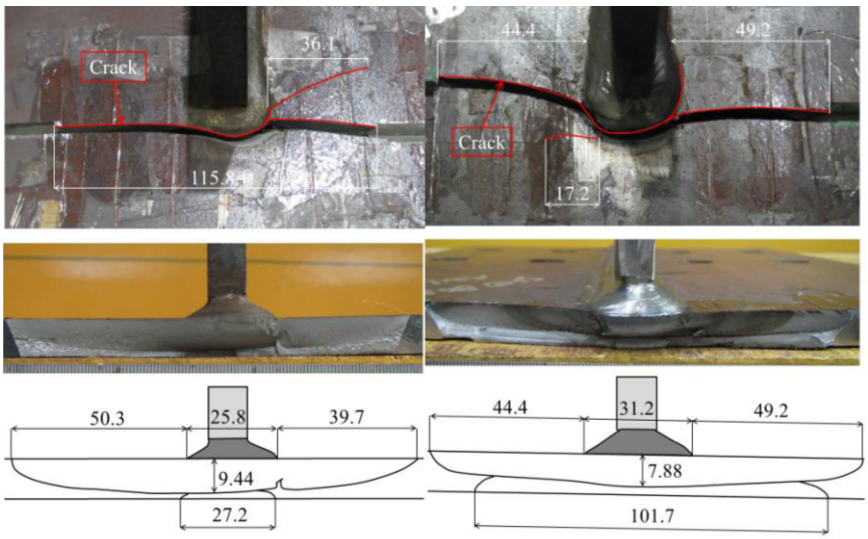

(a)$\Delta\sigma$= 60 N/mm^2 (b) $\Delta\sigma$= 100 N/mm^2

Figure 8. Fracture surface of the AW specimen.

side of the gusset (gages B2 and C2), fatigue crack propagated in the vertical direction against the gusset plate. Thus, the strain ranges at gages B2 and C2 sharply changed with fatigue crack propagation.

In addition, the delamination area of the CFRP plates (dye-marked area) can be observed in Fig. 7. As can be seen in Fig. 7, CFRP plates was delaminated between base plate and adhesive layer. In this study, since the strain ranges at gages C1 and C2 were reduced in all specimens, it can be assumed that CFRP began to delaminate during fatigue tests in all specimens.

As shown in Fig. 6, in the N_{10}+CFRP specimen with "*d*", the strain range at gage C2 located on the CFRP plate, which could not be completely bonded, decreased just after fatigue test started. This implies that the initial delamination of the CFRP plate proceeded just after fatigue test started in the N_{10}+CFRP with "*d*" specimen. The strain range at gage C1 located on the CFRP plate, which can be completely bonded, increased as number of cycles increased and sharply decreased at half million cycles. Therefore, it can be estimated that the CFRP plate began to delaminate at half million cycles. Besides, since the strain range at gage B2 located at the side where the initial adhesive failure was observed is higher than the strain at gage B1 located at the side where the CFRP plate was completely bonded. Accordingly, it seems that the stress at the crack tip could not be completely reduced even if the initial adhesive failure was observed.

3.3. Observation of the fracture surface after fatigue test

3.3.1. AW specimen

Figure 8 shows the fracture surfaces of the AW specimens after fatigue tests. Since the fatigue tests were continued until fatigue cracks propagated to 50mm away from weld toe after fatigue cracks initiated at the back surfaces of the specimen, the fatigue cracks shown in Fig. 8 are longer than those in the fatigue life condition as shown in Fig. 3. In the AW specimen, fatigue crack propagated to the base plate in the vertical direction against the gusset plate under both the stress ranges, $\Delta\sigma$ =60 and 100 N/mm^2.

3.3.2. N_{10}+CFRP specimen

Figure 9 shows the fracture surfaces of the N_{10}+CFRP specimens after fatigue tests. In those specimens, fatigue cracks are also longer than the condition plotted in Fig. 3. In the N_{10}+CFRP specimen, to distinguish the dimensions of the repaired crack, N_{10}, and crack in fatigue life condition, N_t, the repaired crack was dye-marked.

As shown in Fig. 9(a), under the stress range of $\Delta\sigma$= 60 N/mm^2, the repaired crack marked by a broken line re-propagated in the perpendicular direction and diagonal direction against the gusset plate. Finally, the fatigue crack propagated in the diagonal direction against the gusset plate was longer than that in the perpendicular direction against the gusset plate. When CFRP plates are bonded, crack propagation in the perpendicular direction against the gusset plate could be suppressed by the reduction of the longitudinal stress, which is the same as the fiber direction, at the crack tip. On the other hand, it can be assumed that crack propagation in the diagonal direction against the gusset plate was not suppressed because the diagonal stress, which is different direction of fiber, at the crack tip was not decreased. Accordingly, it can be suggested that the fatigue crack will propagate in the diagonal direction against the gusset plate after bonding CFRP plates.

As shown in Fig. 9(b), under the stress range of $\Delta\sigma$= 80 N/mm^2, the repaired crack re-propagated largely in the

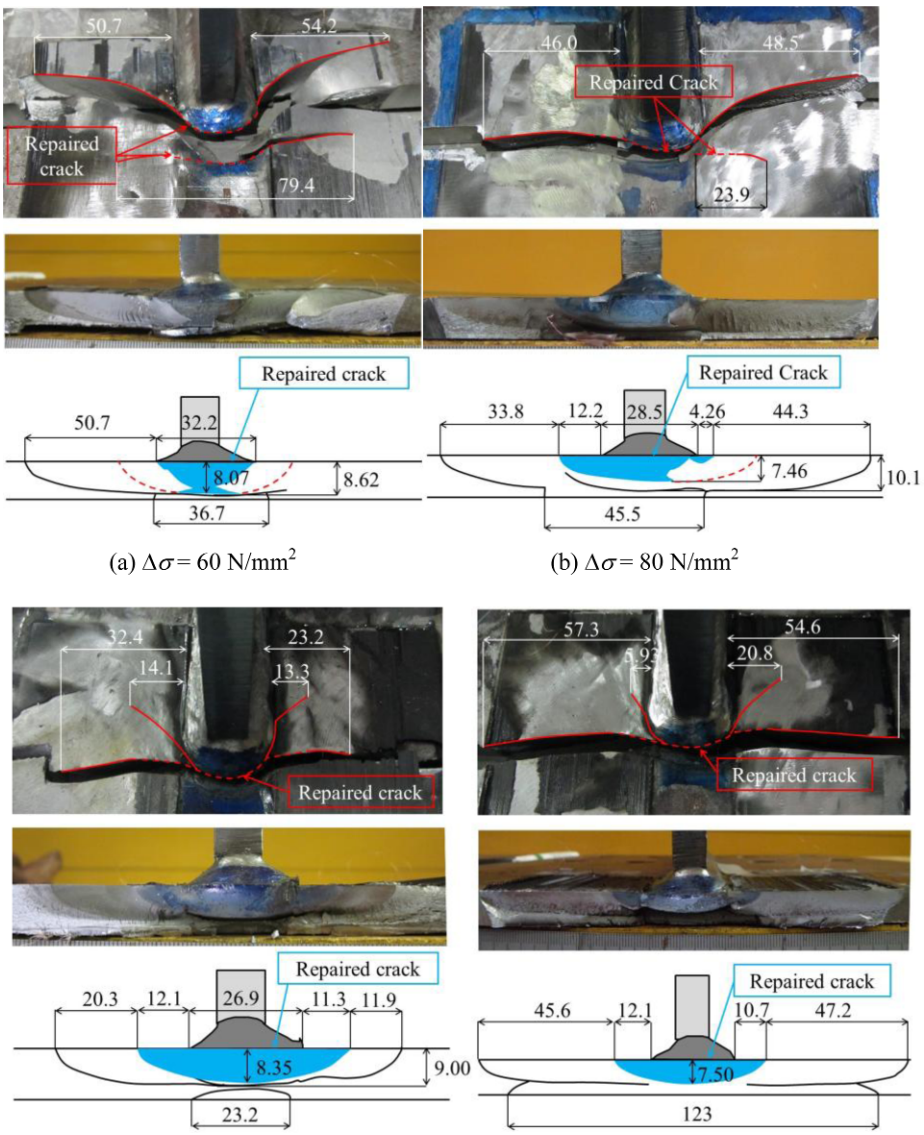

Figure 9. Fracture surface of the N_{10}+CFRP specimen.

diagonal direction against the gusset plate. This shows the same tendency as the stress range of 60 N/mm^2. At the left side of the specimen, the repaired crack re-propagated largely in the perpendicular direction against the gusset plate.

Meanwhile as presented in Fig. 9(c) and 9(d), under the stress ranges of $\Delta\sigma$=100 and 120 N/mm^2, while the repaired cracks propagated in the diagonal direction against the gusset plate were also observed, the crack propagated more largely in the perpendicular direction against the gusset plate. This is because the suppression of crack propagation in the perpendicular direction against the gusset plate is early lost by the small fatigue life of CFRP plate delamination under high stress range.

Accordingly, when fatigue crack was repaired by CFRP plate bonding, the fatigue crack propagated in the perpendicular and diagonal directions against the gusset plate under any stress range. Under the smaller stress ranges of $\Delta\sigma$=60 and 80 N/mm^2, the fatigue crack tends to propagate in the diagonal direction against the gusset plate. On the other hand, under the larger stress ranges of $\Delta\sigma$=100 and 120 N/mm^2, the fatigue crack tends to propagate in the perpendicular direction against the gusset plate. Therefore, future issues are to clarify how long the fatigue lives of cracks propagated in the various directions can be extended by CFRP plates bonding.

4. Fatigue Test Results (stress ratio, *R*= -infinity)

4.1. S-N curve

Fatigue test results are listed in Table 3. Figure 10 shows the stress range versus fatigue life (N_{10}→N_t).

Table 3. Fatigue test results (stress ratio, R= -infinity)

Specimen	State	Stress range (N/mm^2)	Fatigue life N_{10}→N_t (×10^4)
N_{10}+CFRP-1N	N_{10} crack +CFRP	81.7	2110.7*
		99.6	2005.9*
		121.5	186.2
N_{10}+CFRP-2N		97.3	981.2

*: Run-out data

Fatigue tests were conducted under the stress range of $\Delta\sigma$ =80, 100 or 120 N/mm^2 with strass ratio R= -infinity, in each specimen. In the N_{10}+CFRP-1N specimen, since the strain range did not vary during the fatigue test even though number of cycles achieved to 20 million cycles under the stress range of $\Delta\sigma$=80 N/mm^2, the fatigue test was conducted again under the higher stress range of $\Delta\sigma$ =100 N/mm^2. In the higher stress range condition, $\Delta\sigma$= 100 N/mm^2, the strain range did not vary again until 20 million cycles, thus, the stress range was set to 120 N/ mm^2. In Fig. 10, fatigue lives of CFRP plate delamination are also plotted as open circles. In this figure, a regression line of fatigue lives of CFRP plate delamination under stress ratio, R=0, is shown as a broken line. In case of stress ratio, R= -infinity, under the stress range of $\Delta\sigma$= 100 N/mm^2, the delamination of the CFRP plate was not be observed. On the contrary, under the stress range of $\Delta\sigma$ =120N/mm^2, the fatigue crack initiated at the back surface of the specimen after the CFRP plate began to delaminate. This shows the same tendency as fatigue test results with stress ratio R=0. As can be seen in Fig. 10, fatigue lives of the specimens repaired with the CFRP plates could be extended more than 10 times longer than those of the specimens in as-welded conditions. Therefore, it can be estimated that the repair method for fatigue crack by CFRP bonding under the stress ratio R= -infinity is more effective than that under the stress ratio R=0. This is because the fatigue test data under stress ratio R = -infinity showed much longer fatigue lives of CFRP plate delamination compared with that under stress ratio, R=0. Additionally, in Fig. 10, the fatigue lives of the N_{10}+SH specimens in which N_{10} crack is repaired by stop holes are also plotted (Matsumoto *et al*., 2016). The fatigue life of the N_{10}+SH specimen is defined as the number of cycles after the stop holes are drilled at the crack tip until fatigue crack propagated to 1mm away from stop hole edge. As can be seen in Fig. 10, the N_{10}+CFRP specimen showed fatigue life extension equal to or larger than the N_{10}+SH specimen. Therefore, it can be clarified that the bonding CFRP plates on cracks is effective as a tentative repair method for fatigue crack.

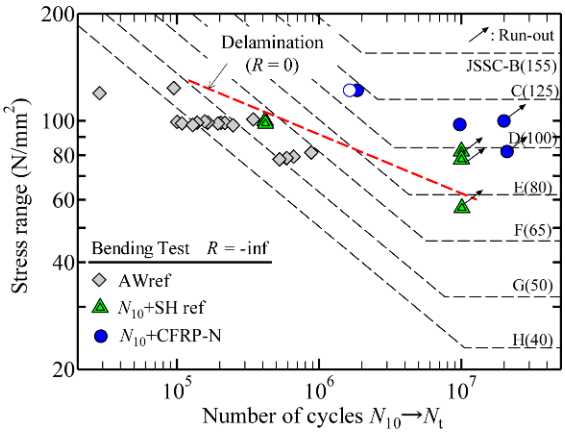

Figure 10. S-N curve (stress ratio, R= -infinity)

4.2. Variation of strain range during fatigue test

Variation of the strain range during fatigue tests are shown in Figs. 11 and 12. In Figs. 11 and 12, the strain ranges of the AW specimen under N_{10} condition at gages A, B1 and B2 (AW, N_{10}), which are the strain ranges measured at the same specimen just before bonding CFRP plates, are also plotted as broken lines.

As shown in Fig. 11(a), in the N_{10}+CFRP-1N specimen

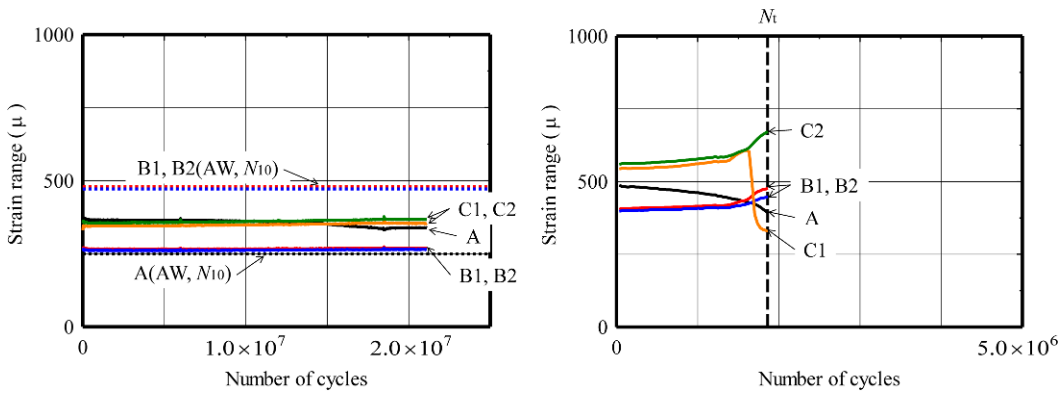

(a) $\Delta\sigma$= 80 N/mm^2 (b) $\Delta\sigma$= 120 N/mm^2

Figure 11. Variation of strain range in the N_{10}+CFRP-1N specimen.

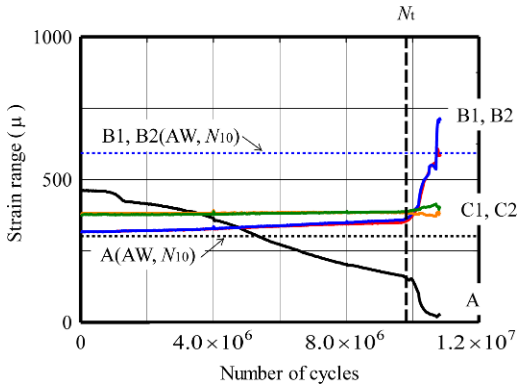

Figure 12. Variation of strain range in the N_{10}+CFRP-2N specimen ($\Delta\sigma$=100 N/mm^2).

under the stress range of $\Delta\sigma$=80 N/mm^2, the strain ranges at gages B1 and B2 located at the crack tips became half of those in the AW specimen under N_{10} condition (AW, N_{10}). Accordingly, the stresses at the crack tips could be reduced by the CFRP bonding. On the other hand, the strain range at gage A located near the weld toe in the N_{10}+CFRP-1N specimen was larger than that under (AW, N_{10}) condition. This shows the different tendency from the case of stress ratio R=0. To clarify this difference, the fracture surface of the N_{10}+CFRP-1N specimen after fatigue test was investigated as shown in Fig. 13. As shown in Fig. 13, the adhesion bond was penetrated to the repaired crack in the N_{10}+CFRP-1N specimen. Accordingly, it can be assumed that the strain range at gage A increased by bonding CFRP, since the stress generated in base plate could become transferred to the weld toe via

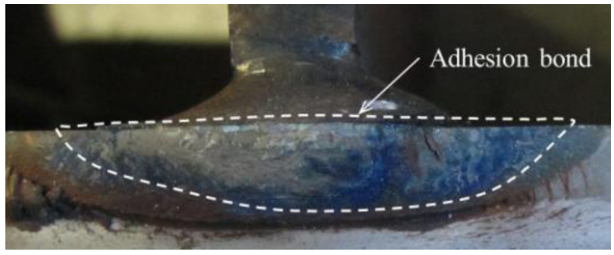

Figure 13. Adhesion bond penetrated into the crack.

the adhesion bond penetrated into the crack under stress ratio R= -infinity. From Fig. 11(a), the strain range at gage A decreased slightly with increase of number of cycles and variation of the strain range at gage A converged at 17 million cycles under the stress range of $\Delta\sigma$=80 N/mm^2. Additionally, the strain ranges at gages B1, B2, C1 and C2 were almost constant during the fatigue test. Hence, it can be assumed that the fatigue crack did not re-propagate under the stress range of $\Delta\sigma$=80 N/mm^2.

As shown in Fig. 11(b), in the N_{10}+CFRP-1N specimen under the stress range of $\Delta\sigma$=120 N/mm^2, since the strain range at gage A decreased and the strain ranges at gages B1 and B2 increased with increase of number of cycles, it seems that the fatigue crack re-propagated under the CFRP plates. At gages C1 and C2, although the strain ranges increased with fatigue crack propagation, the strain ranges dropped sharply at 1.6 million cycles. Therefore, the CFRP plates began to delaminate when the number of cycles reached to 1.6 million cycles.

As shown in Fig. 12, in the N_{10}+CFRP-2N under the stress range of $\Delta\sigma$=100 N/mm^2, since the strain range at

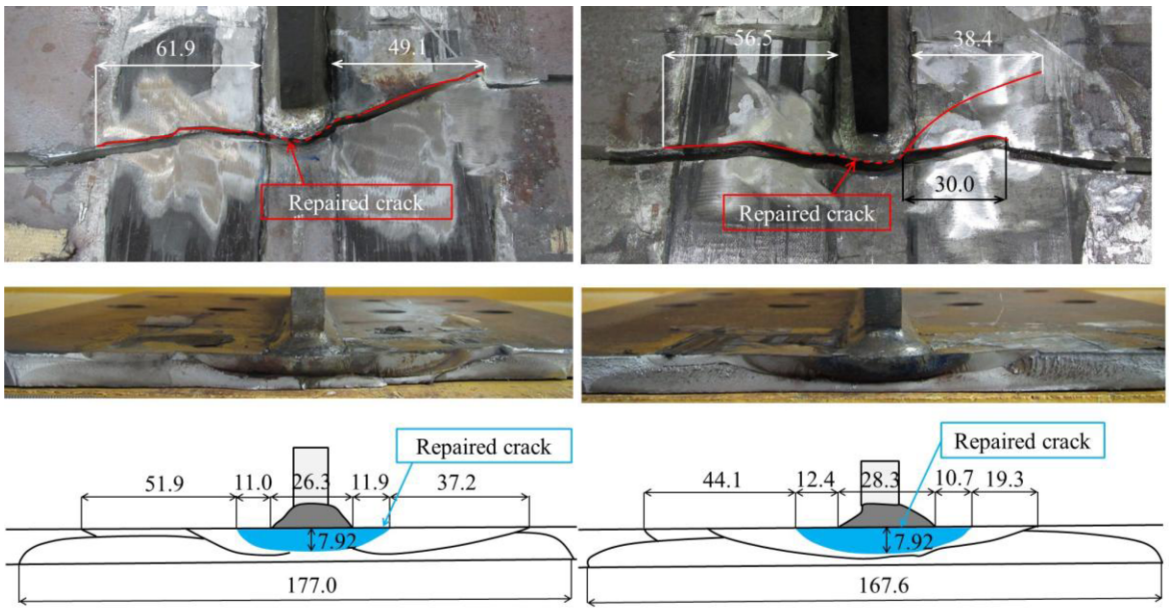

(a) N_{10}+CFRP-1N ($\Delta\sigma$= 120N/mm^2) (b) N_{10}+CFRP-2N ($\Delta\sigma$= 100N/mm^2)

Figure 14. Fracture surface of the N_{10}+CFRP

gage A decreased and the strain ranges at gages B1 and B2 increased as number of cycles increased, it can be assumed that the fatigue crack re-propagated. Furthermore, the strain range at gage A sharply decreased and the strain ranges at gages B1 and B2 increased after fatigue crack initiated at the back surface of the specimen. Therefore, it seems that the crack propagation velocity accelerated just after fatigue crack initiated at the back surface of the specimens. Nevertheless, since the strain ranges at gages C1 and C2 located on the CFRP plates did not vary during fatigue test, it can be assumed that the CFRP plates did not delaminate during fatigue test. Accordingly, it was clarified that the CFRP plate did not delaminate under the stress range of less than 100 N/mm^2.

4.3. Observation of fracture surfaces in specimen after fatigue test

Figure 14 shows the fracture surfaces of the N_{10}+CFRP-N specimens after fatigue tests finished. From this figure, the fatigue crack lengths were longer than that in fatigue life condition, because the fatigue tests were continued after fatigue cracks initiated at the back surface of the specimen.

As shown in Fig. 14(a), in the N_{10}+CFRP-1N specimen under the stress range of $\Delta\sigma$=120 N/mm^2, the fatigue crack propagated in the perpendicular direction against the gusset plate. On the other hand, in the N_{10}+CFRP-2N specimen under the stress range of $\Delta\sigma$=100 N/mm^2, the fatigue crack propagated in the several directions and finally fatigue crack mainly propagated in the diagonal direction against the gusset plate. The direction of the crack propagation under stress ratio R= -infinity shows the same tendency as that under stress ratio R=0.

5. Conclusions

In this study, the effect of bonding CFRP plates on fatigue life extension under bending was clarified by bending fatigue tests. The main conclusions are as follows:

(1) Under stress ratio R=0, and the stress ranges of 60 to 120 N/mm^2, fatigue life of the specimen repaired by CFRP bonding extended more than 4 times longer than that of the as-welded condition, even if they have partially delamination of the CFRP plate during fatigue test.

(2) Under stress ratio R=0, the fatigue crack re-propagated in the perpendicular and diagonal directions against the gusset plate in the specimen repaired by CFRP bonding. Under the smaller stress ranges of 60 and 80 N/mm^2, the fatigue crack re-propagated in the diagonal direction. On the contrary, under the higher stress ranges of 100 and 120 N/mm^2, the fatigue crack re-propagated in the perpendicular direction against the gusset plate.

(3) Under the stress ratio R= -infinity, and the stress ranges of 80 to 120 N/mm^2, fatigue life of the specimen repaired by CFRP bonding extended more than 10 times longer than that of the specimen in as-welded condition. Furthermore, CFRP did not delaminate under the stress ranges of less than 100 N/mm^2.

(4) Under the stress ratio R= -infinity, and the stress ranges of less than 100 N/mm^2, the fatigue crack re-propagated in the diagonal direction. Under the stress range of 120 N/mm^2, the fatigue crack re-propagated in the perpendicular direction against the gusset plate.

References

Chacon, A., Chajes, M. J., Richardson, D. and Wenczel, G. (2004). "Applications of Advanced Composites to Steel Bridges a Case Study on the Ashland Bridge (Delaware-USA)", *Proceedings of the 4th International Conference on Advanced Composite Materials in Bridges and Structures*, Calgary, Canada, pp. 8.

Colombi, P. (2005). "Plasticity induced fatigue crack growth retardation model for steel elements reinforced by composite patch", *Theoretical and Applied Fracture Mechanics*, Vol.43, pp. 63-76.

Liu, H., Xiao, Z., Zhao, X. L. and Al-Mahaidi, R. (2009). "Prediction of fatigue life for CFRP-strengthened steel plates", *Thin Welled Structures*, Vol.47, Isuue 10, pp. 1069-1077.

Matsumoto, R., Ishikawa, T., Tsukamoto, S., Awazu, Y. and Kawano, H. (2016) "Comparison of repair methods for fatigue crack initiated at welded toe between steel deck plate and vertical stiffener", *Journal of Japan Society of Civil Engineers, Ser. A1 (Structural Engineering & Earthquake Engineering (SE/EE))*, Vol. 72, No. 1, pp. 192-205.

Nakamura, H., W. Jiang, Maeda, K., Suzuki, H., Irube, T. and Fukuda, Y. (2011) "Fatigue Life Prediction for Fatigue Crack at Out-of-Plane Welded Gusset Joint Repaired with CFRP Strips", *Journal of Structural Engineering A*, Vol. 57A, pp. 842-851. (in Japanese)

National Research Council-Advisory Committee on Technical Recommendations for Construction (2007). "Guidelines for the Design and Construction of Externally Bonded FRP Systems for Strengthening Existing Structures", CNR-DT 202/2005.

Phares, B. M., Wipf, T. J., Klaiber, F. W., Abu-Hawash, A. and Lee, Y. S. (2003). "Strengthening of Steel Girder Bridges Using FRP", *Proceedings of the 2003 Mid-Continent Transportation Research Symposium*.

Roach, D., Rackow, K., Delong, W. and Franks, E. (2008). "In-Situ Repair of Steel Bridges Using Advanced Composite Materials, International Bridge and Structure Management", *10th International Conference on Bridge and Structure Management, Transportation Research Circular E-C128*, pp. 269-285.